Facile assembly of micro- and nanoarrays for sensing with natural cell membranes

*Nathan J. Wittenberg[1], Hyungsoon Im[1], Timothy W. Johnson[1], Xiaohua Xu[2], Arthur E. Warrington[2], Moses Rodriguez[2] and Sang-Hyun Oh[1]**

[1]Department of Electrical and Computer Engineering, University of Minnesota, Twin Cities, MN, U.S.A.

[1]Departments of Neurology and Immunology, Mayo Clinic College of Medicine, Rochester, MN, U.S.A.

*Correspondence: sang@umn.edu

Supporting Information

Comparison of fluorescence and vesicle surface area distributions: The distribution of fluorescence intensity from microwells shown in Figure 2c represents the distribution of the total amount of membrane material in the wells, since all vesicles are assumed to contain the same proportion of fluorescent lipid. Broken down further, this distribution is a combination of two separate distributions: the distribution of the number of vesicles per well and the distribution of surface area of those vesicles. Also plotted in Figure 2c is the distribution of surface area (determined by dynamic light scattering (DLS)) for vesicles in solution after extrusion through 200 nm pores. Vesicle diameter from DLS is converted to surface area by assuming the vesicles are spherical. Because we assume that the number of fluorophores per unit is the same for all vesicles, the fluorescence intensity of an individual vesicle should scale linearly with its surface area. If a vesicle array was composed only of individual intact vesicles, the distribution of fluorescence intensity would exactly match the distribution of surface area if both were plotted against deviation from the mean. Figure 2c shows that the two distributions are quite similar. In fact, the full width at half maximum (FWHM) of the fluorescence distribution is slightly narrower than the FWHM of the surface area distribution (2.2 standard deviation units vs. 2.4 standard deviation units). This indicates that the amount of lipid material in the microwells is no more heterogeneous than the surface areas of the same vesicles free in solution. In essence, this means that these arrays are no less uniform, with respect to the amount of lipid per individual array well, than if the array had one vesicle per well.

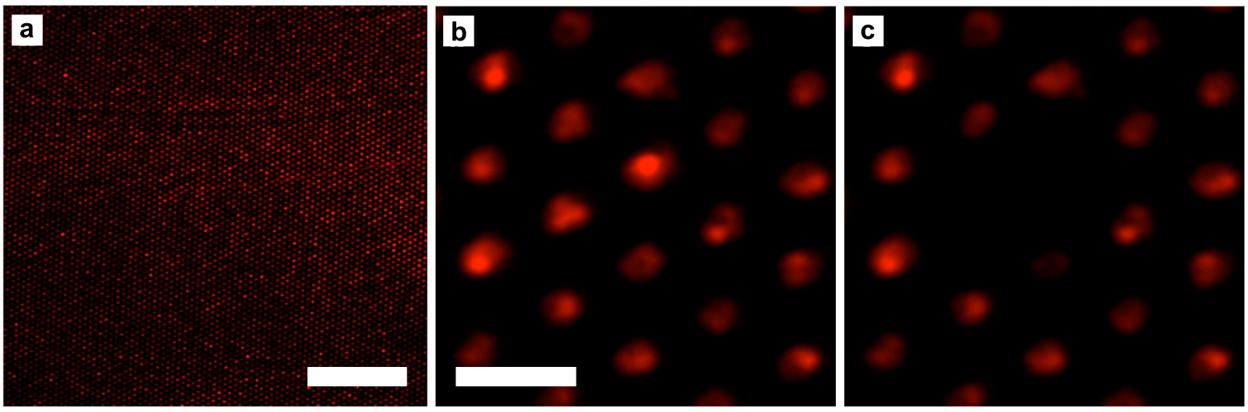

Figure S1. (a) Large area (212 x 212 μm) membrane microarray formed by directed assembly of egg PC vesicles containing 1% rhodamine-B-labeled phosphatidylethanolamine (Rho-PE) The scale bar is 50 μm. (b-c) Photobleaching of 2 wells of a membrane microarray of egg PC/1% Rho-PE. The wells are 1 μm in diameter with 3 μm periodicity. (b) Image taken prior to photobleaching. The scale bar is 5 μm. (c) Image taken 2 minutes after photobleaching. There is no recovery of fluorescence in the two wells, indicating that no supported lipid bilayer is formed and that there is no diffusive transport of material between the microwells, even over short distances. The scale bar in (b) also applies to (c).

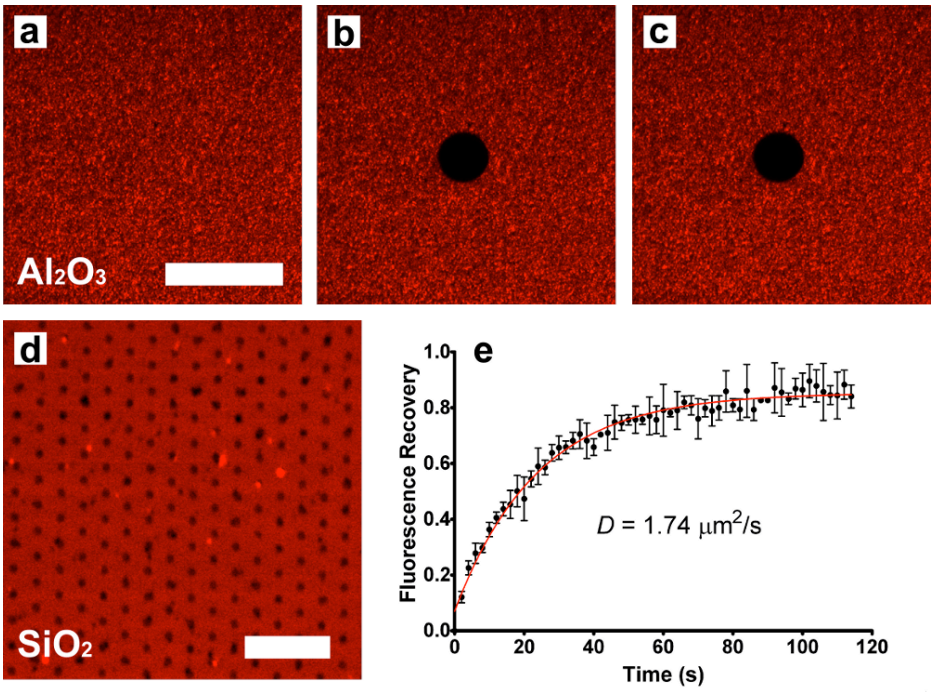

Figure S2. Photobleaching of vesicles and supported lipid bilayers on Al_2O_3 and SiO_2-coated microwell arrays. (a) Fluorescence image of a microwell array (1 μm hole diameter, 3 μm periodicity) with adsorbed vesicles composed of egg PC and 1% Rho-PE. The array is not readily visible because the vesicles uniformly cover the surface and the substrate had not been passed over with the PDMS squeegee. The scale bar is 30 μm and applies to (b) and (c) as well. (b) Fluorescence image of the same area as in (a) immediately after being exposed to a focused laser beam (405 nm) for 20 seconds. (c) The same area as in (a) and (b) 2 minutes after the photobleaching laser pulse showing that there is no fluorescence recovery. This suggests that the vesicles do not spontaneously rupture to form a supported lipid bilayer on Al_2O_3. (d) Fluorescence image of a SiO_2-coated microwell array (1 μm hole size, 3 μm periodicity) showing the formation of a supported lipid bilayer on the surface. The dark areas are the microwells, indicating that the supported lipid bilayer does not span the wells coplanar with the substrate surface. The scale bar is 10 μm. (e) Average fluorescence recovery curve and single exponential fit on SiO_2 showing that fluorescence recovers after photobleaching. The calculated diffusion coefficient of the lipids in the bilayer is 1.74 $\mu m^2/s$. The average is from 3 separate experiments and the error bars represent the standard deviations of the individual data points.

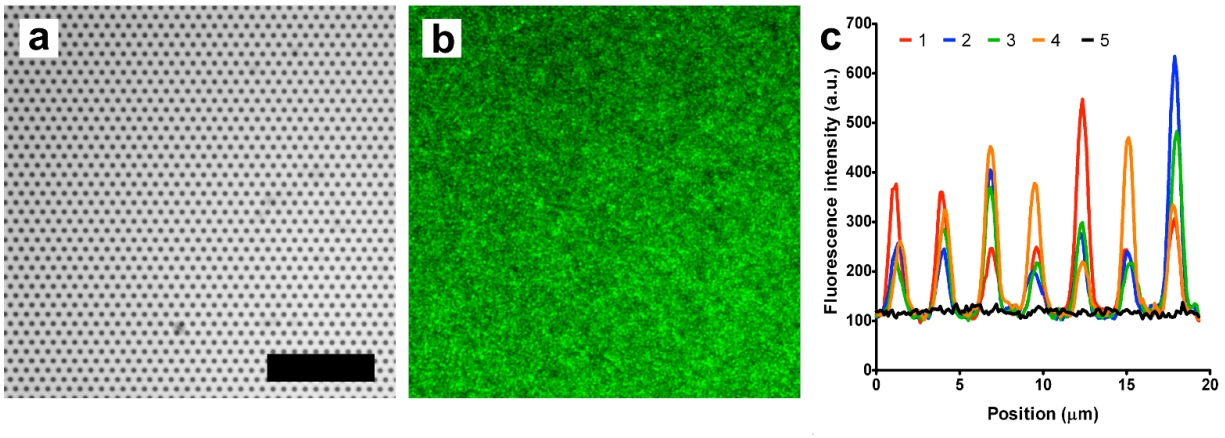

Figure S3. (a) A bright field image of a microarray with 1 μm-diameter wells with 3 μm periodicity. (b) The same array as in (a) after coverage with FM1-43 stained lipid rafts showing uniform coverage. The image was taken before application of the PDMS squeegee. The scale bars in (a) is 30 μm and applies to (b) as well. (c) Fluorescence intensity profiles from lines 1 – 5 shown in Figure 3c of the manuscript.

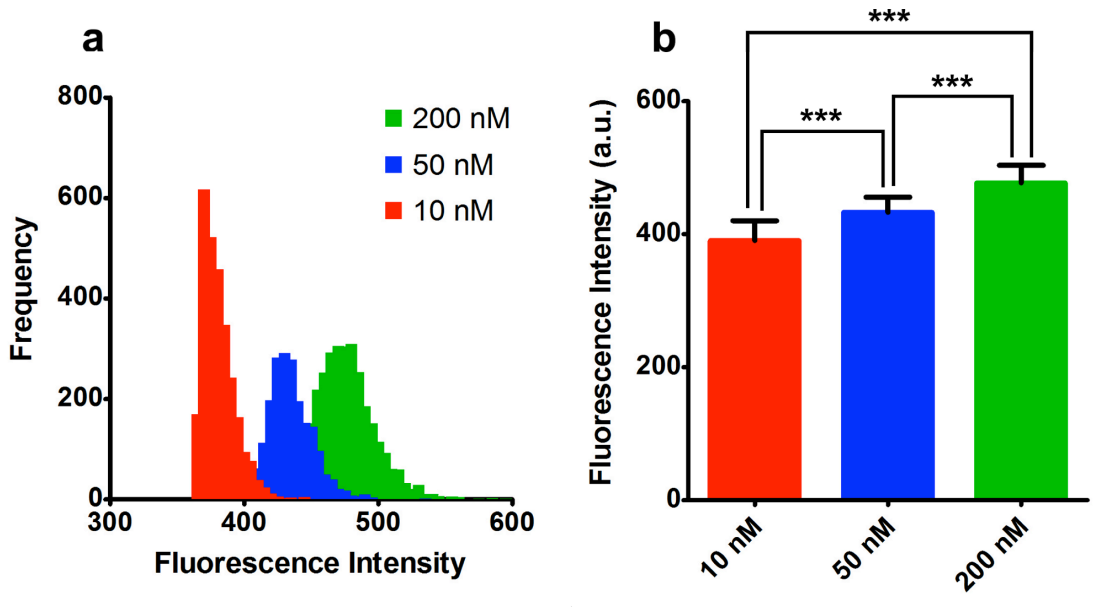

Figure S4. (a) Histograms of fluorescence intensities for individual array spots incubated with 10, 50 and 200 nM cholera toxin (CTX) showing that the distributions shift to larger values with increasing CTX concentration. (b) Comparison of mean fluorescence intensities for individual lipid raft array spots incubated with 10, 50 and 200 nM CTX. The error bars are standard deviations. The number of individual array spots analyzed for the three concentrations were $N_{10\ nM} = 2794$, $N_{50\ nM} = 2160$ and $N_{200\ nM} = 3108$. The means were determined to be significantly different using one-way ANOVA (Kruskal – Wallis test) and post-hoc testing (Dunn's Multiple Comparison test). *** indicates a P value of < 0.001.

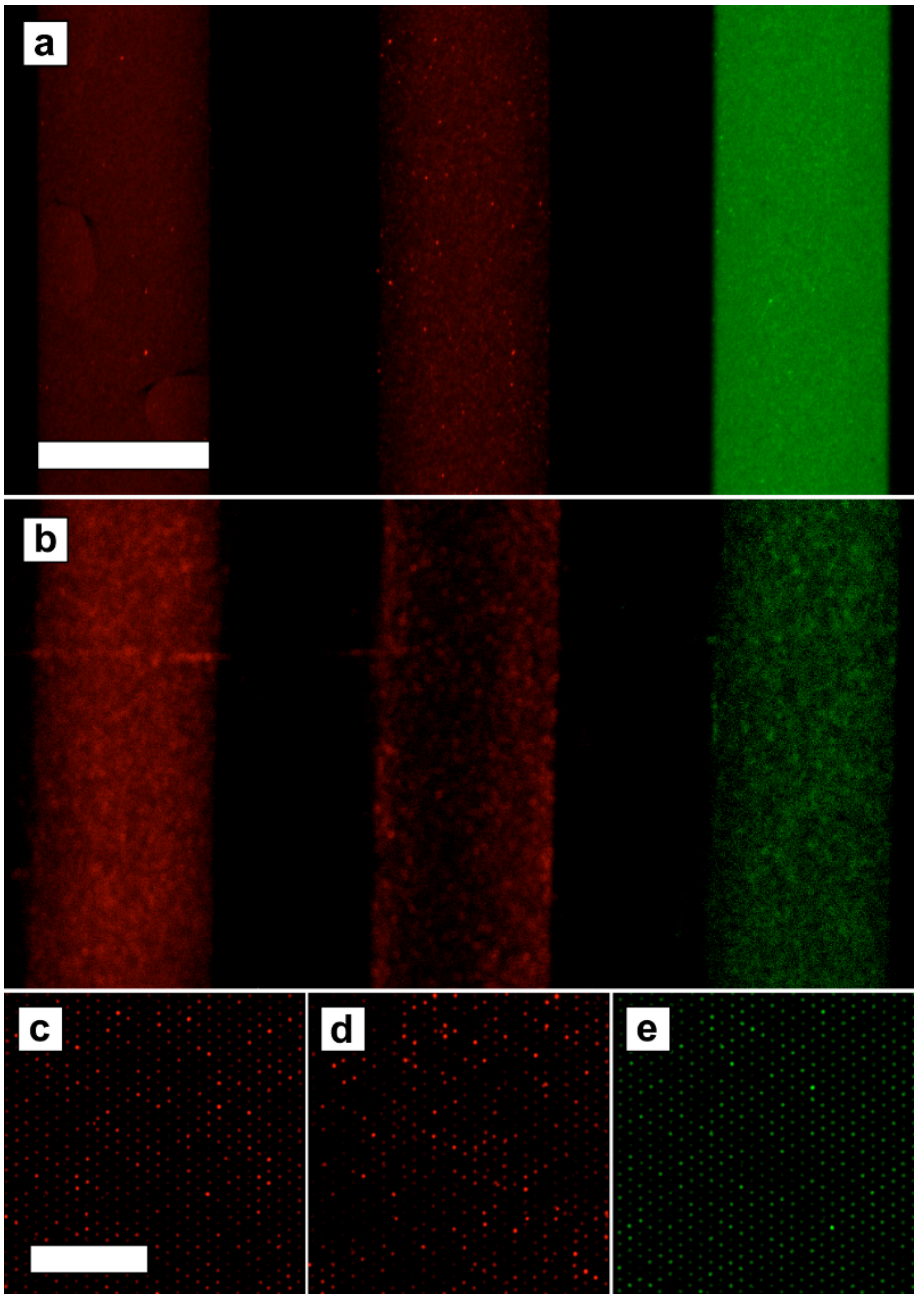

Figure S5. Multicomponent vesicle array formed by microfluidic delivery of vesicles. (a) Immobilized fluorescent vesicles inside the microfluidic channels before using the PDMS squeegee to form microarray stripes. The left and center channels contain egg PC vesicles labeled with Rho-PE, while the right channel contains egg PC vesicles labeled with NBD-PE. The scale bar is 250 μm. (b) Microarray stripes formed after detaching the microfluidic and using the PDMS squeegee. (c-e) Zoomed in images of the left, center and right stripes showing the individual array spots. The scale bar is 30 μm and applies to (c-e)

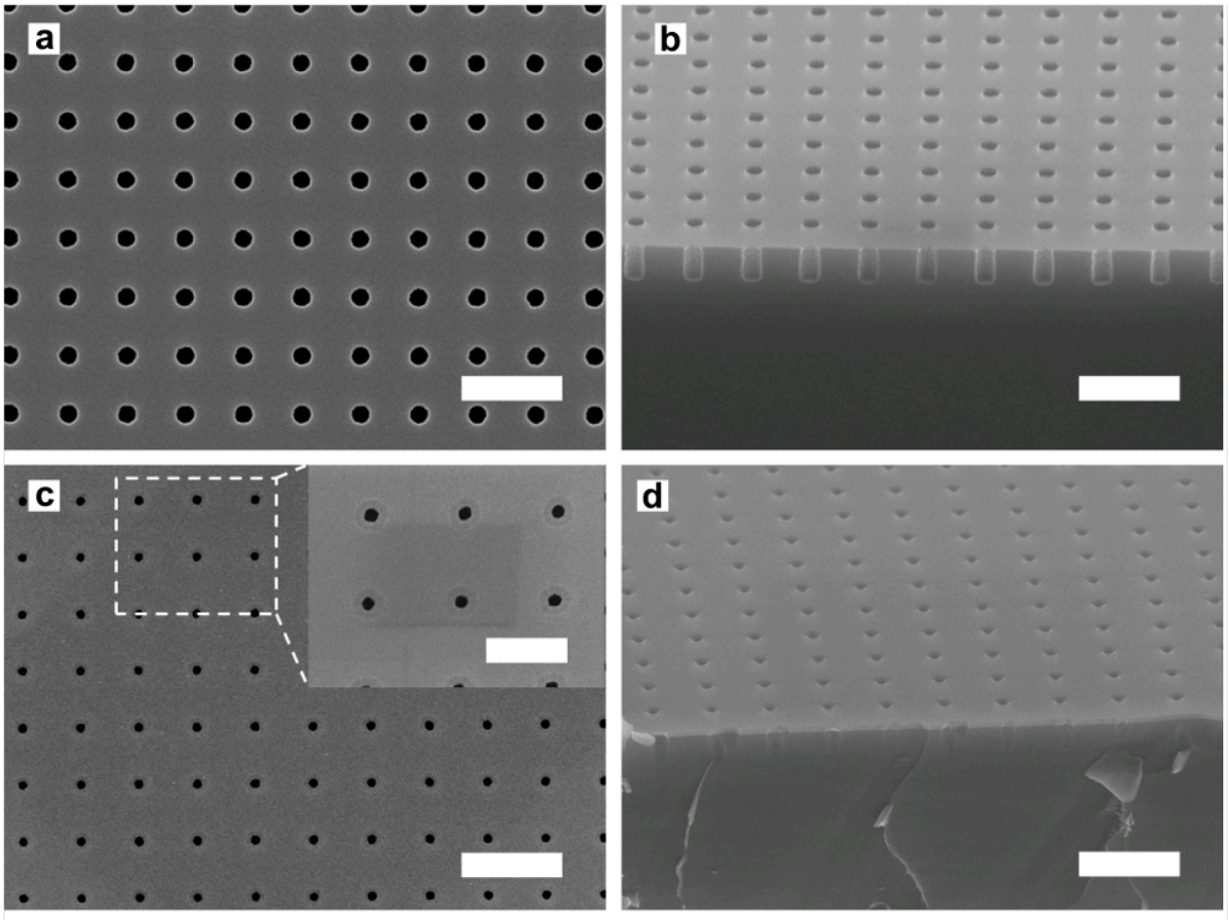

Figure S6. Nanowell arrays showing the tunability of well size with atomic layer deposition of Al_2O_3. The initial pore size in the silicon wafer is 200 nm and the periodicity is 600 nm., Deposition of various thicknesses of Al_2O_3 effectively reduces the diameter due to conformal deposition. (a) Top view of a nanowell array with well diameter of 180 nm. (b) Cross-sectional view of a nanowell array with well diameter of 180 nm. (c) Top view of a nanowell array with a well diameter of 80 nm. The inset is an image of the same array at a higher magnification. Notice the faint rings surrounding the dark wells. This is the Al_2O_3 layer. (d) Cross-sectional view of a nanowell array with a well diameter 80 nm. The lighter color top layer in the cross section is Al_2O_3. The scale bars in (a-d) are 1 μm and the scale bar in (c, inset) is 500 nm.

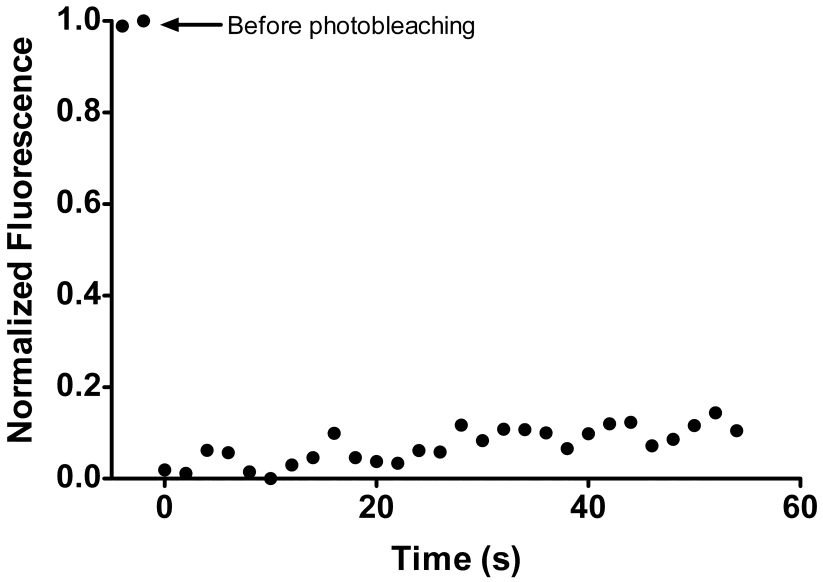

Figure S7. Normalized fluorescence from vesicles immobilized in an array of 80 nm diameter wells before and after photobleaching.

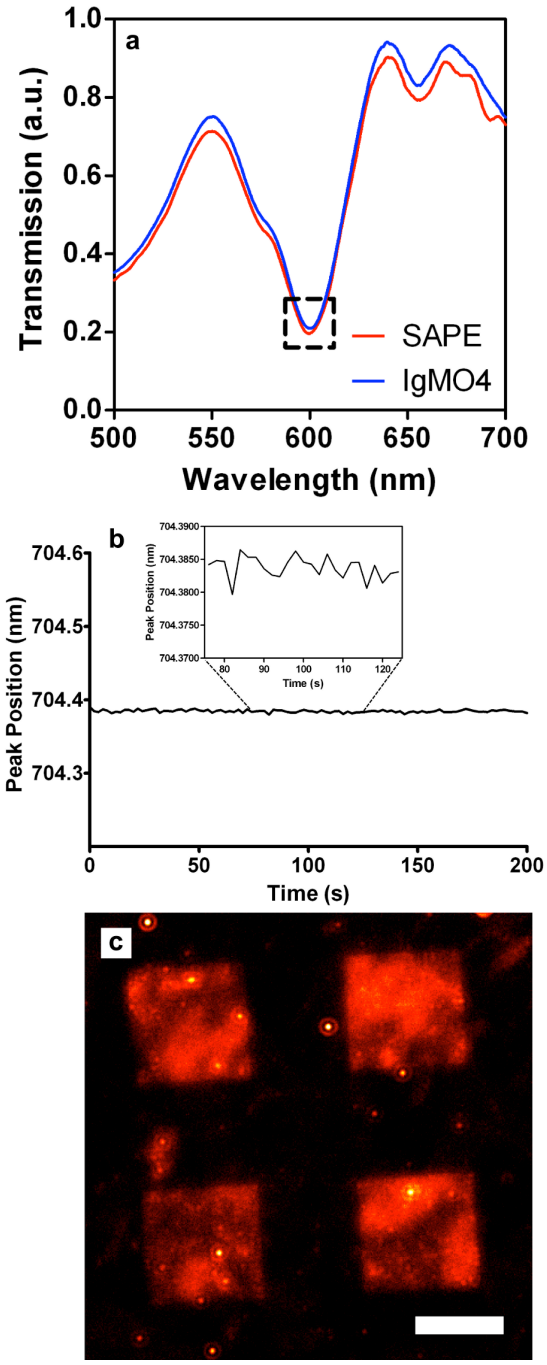

Figure S8. (a) Spectra of visible light transmission through gold nanowell arrays after exposure to SAPE (red curve) and IgMO4 (blue curve). The area marked by the dashed box is shown in Figure 5e in the manuscript. (b) Continuous monitoring of a peak in the transmission spectrum as a function of time to determine the noise level associated with the SPR measurements. The inset is a zoomed in view of the segment from 75 – 125 seconds. The standard deviation of the noise is 1.78×10^{-3} nm. (c) Fluorescence image of IgMO4 bound to myelin particles immobilized in gold nanowell arrays. Scale bar = 10 μm.

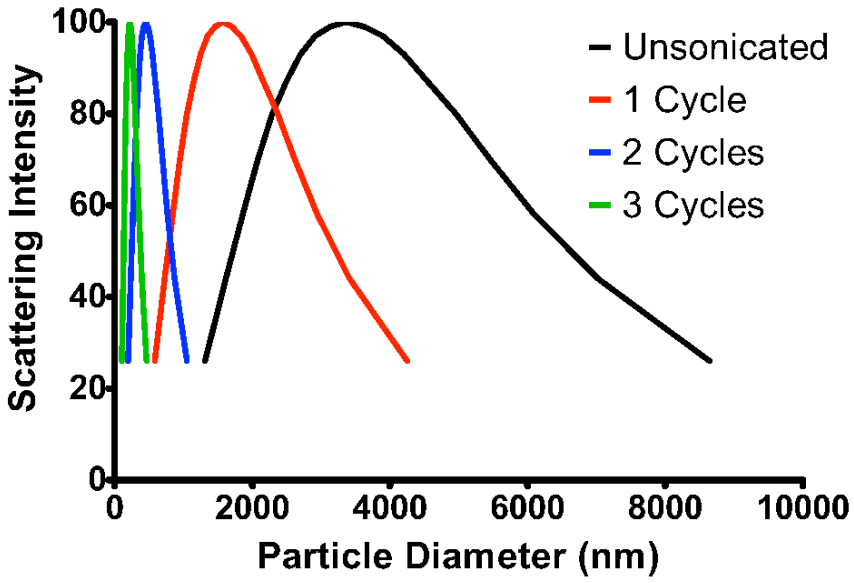

Figure S9. Dynamic light scattering results showing myelin particle size distribution after being subjected to 1, 2, or 3 15-minute rounds of sonication. A control that was not subjected to sonication was analyzed as well. The particle size distribution centers were 3.369 ± 0.002 μm, 1.576 ± 0.001 μm, 451.4 ± 0.3 nm and 220.3 ± 0.1 nm (distribution center ± standard error of center) for samples sonicated 0, 1, 2 and 3 times, respectively. The distribution center and standard error of the center were determined by fitting the distributions to log Gaussian curves.